Title
INTENSE, MIXED-ENERGY HYDROGEN BEAMS FOR CTR INJECTION

Authors
Berkner, Klaus H.
Pyle, Robert V.
Stearns, J. Warren.

Publication Date
1974-06-01

Submitted to Nuclear Fusion

LBL-3053
Preprint

INTENSE, MIXED-ENERGY HYDROGEN BEAMS FOR CTR INJECTION

Klaus H. Berkner, Robert V. Pyle and J. Warren Stearns

June 1974

Prepared for the U. S. Atomic Energy Commission
under Contract W-7405-ENG-48

DISCLAIMER

INTENSE, MIXED-ENERGY HYDROGEN BEAMS FOR CTR INJECTION*

Klaus H. Berkner, Robert V. Pyle, and J. Warren Stearns

Lawrence Berkeley Laboratory
University of California
Berkeley, California 94720

June 1974

ABSTRACT

Present high-current ion sources for neutral injection experiments accelerate a mixture of atomic and molecular hydrogen species that are converted into neutral particles with different energies and neutralization efficiencies. Beam composition can have important effects on injection system efficiency, vacuum design, and first-wall loading. Beam composition measurements of the 20-keV LBL high-current sources are used to calculate the relative power in the various beam components expected at higher energies.

1. INTRODUCTION

Neutral-beam systems, now under discussion for fusion experiments and reactors, will require tens to hundreds of megawatts of electrical power. The choice and control of the atomic and molecular ion species in the plasma source can have an important effect on the capital and operating costs, with or without recovery of the energy of the non-neutralized fraction of the beam. (In the former case, electrostatic energy recovery from a poly-energetic ion beam would cause additional complexity.) The required amount of cold gas in the neutralizing cell varies with energy and species, and in turn affects the cost of the large vacuum system. Neutrals with different energies will be trapped at different plasma radii; in particular, low-energy atoms will be trapped at large radii and increase the power loading on limiters and first walls. For the hydrogen beams discussed in this paper, the trapping of an injected H_2 or D_2 molecule produces (by dissociation) an energetic atom that may escape to the wall. Helium atoms may also be used for heating and fueling of CTR plasmas; this topic is not discussed here.

2. BEAM SPECIES AND NEUTRALIZATION

Ions in a hydrogen, deuterium, or tritium discharge exist principally in four forms, for example D^+, D_2^+, D_3^+, and D^-. Each of these ions, when extracted from the plasma and accelerated to form a high-energy beam, may be electrically neutralized in part by capturing an electron from a neutral gas target, by dissociation, or by losing an electron to the target. For collisionally thick targets, the competition between electron-capture-and-loss collisions establishes an equilibrium balance of positive, negative, and neutral particles in the emerging beam.

For a beam which contains no molecular ions, the collision-induced changes in the various charge states of the beam are described by the set of equations

$$\frac{dF_i}{d\pi} = \sum_{j\neq i} F_j \sigma_{j,i} - F_i \sum_{j\neq i} \sigma_{i,j} \qquad i,j = D^+, D^0, D^-, \qquad (1)$$

where F_i is the fraction of the beam in charge state i, $\sigma_{i,j}$ is the cross section for a collision in which the energetic particle changes its charge from i to j, and π is the target line density of the neutralizer (molecules/cm^2).

For a beam of diatomic molecules there are two such sets of equations, one for the molecular species and another for the atomic dissociation fragments at one-half the molecular energy:

$$\frac{dF_k}{d\pi} = F_\ell \sigma_{\ell,k} - F_k(\sigma_{k,\ell} + \frac{1}{2} \sum_i \sigma_{k,i}) \qquad k,\ell = D_2^+, D_2^0$$

$$\frac{dF_i}{d\pi} = \sum_{j\neq i} F_j \sigma_{j,i} - F_i \sum_{j\neq i} \sigma_{i,j} + \sum_k F_k \sigma_{k,i} \qquad i,j = D^+, D^0, D^- . \qquad (2)$$

Here $\sigma_{k,i}$ is the cross section for the production of the atomic species i from the molecular species k (e.g., production of D^0 from D_2^+). Since two atomic species result from the dissociation of one diatomic molecule, this definition of $\sigma_{k,i}$ yields the factor 1/2 in the molecular equation.

Likewise, for an initial beam of D_3^+ ions, there is one equation for the triatomic molecular ions (there is no reliable evidence of a stable

D_3^0 molecule), a set of equations for the diatomic molecular dissociation fragments at 2/3 of the D_3^+ energy, and a third set for the atomic fragments at 1/3 of the D_3^+ energy:

$$\frac{dF_{D_3^+}}{d\pi} = - F_{D_3^+} \left(\frac{1}{3} \sum_i \sigma_{D_3^+,i} + \frac{2}{3} \sum_k \sigma_{D_3^+,k} \right)$$

$$\frac{dF_k}{d\pi} = F_\ell \sigma_{\ell,k} - F_k (\sigma_{k,\ell} + \frac{1}{2} \sum_i \sigma_{k,i}) + F_{D_3^+} \sigma_{D_3^+,k} \qquad \begin{matrix} k,\ell = D_2^+, D_2^0 \\ i,j = D^+, D^0, D^- \end{matrix}$$

$$\frac{dF_i}{d\pi} = \sum_{j \neq i} F_j \sigma_{j,i} - F_i \sum_{j \neq i} \sigma_{i,j} + \sum_k F_k \sigma_{k,i} + F_{D_3^+} \sigma_{D_3^+,i} \,. \qquad (3)$$

It is clear that for a particular neutralizer a host of cross-section data is required to determine the neutralization efficiency. These data are not always available for an arbitrary choice of neutralizers, so it is not possible at this time to do a systematic study. Enough sample calculations have been carried out, however, to indicate that D_2 is representative of the better gas neutralizers. (For D^- and the molecular ions, plasma targets should be more efficient than gas neutralizers [1]. Such targets have not been tried yet and will not be discussed here.) Our choice of the appropriate cross sections for D_2, gleaned from the literature, is given in Table I. The cross sections and the uncertainty estimates in Table I are based on comparisons of various published values [2] of the same quantities, and on interpolations or extrapolations if no measurements exist; they are not to be considered "best values", i.e., no evaluations of the various experiments have

been made. (Note that most cross sections are not known very accurately.)

As an example appropriate to energies assumed in calculations for two-component experiments, the neutralization efficiency vs D_2 target thickness obtained from Eqs. (1), (2), and (3) is shown in Fig. 1 for 200 keV/deuteron beams (200-keV D^+ and D^-, 400-keV D_2^+, and 600-keV D_3^+). The horizontal scale is the target thickness for a D_2 neutralizer. The logarithmic vertical scale is the neutral power conversion efficiency, η[(power in neutral beam)/(power in incident ion beam)]. For the incident molecular ions the power in the neutral beam is obtained by summing the contributions from 200-keV D^0 and 400-keV D_2^0. The maxima at intermediate neutralizer thickness in the molecular-ion curves of Fig. 1 result from the presence of D_2^0 molecules which exist at low target thicknesses but are destroyed by dissociation in thick targets. These maxima become less pronounced at lower energies and disappear below about 130 keV/deuteron. At even lower energies (below about 75 keV/deuteron) the η vs π curves for the molecular ions lie below the D^+ curve, i.e., low-energy molecular-ion beams require larger values of π than do D^+ beams to achieve the same neutralization efficiencies.

The maximum neutralization efficiency as a function of energy for each species is shown in Fig. 2. At low energies, each beam produces the same result. It is only above 75 keV that D^- starts to show any advantage, and above 130 keV/deuteron that D_3^+ or D_2^+ beams produce more neutral power than D^+. The molecular ions, of course, require higher acceleration voltages.

In choosing a neutralizer for an injection experiment one must compromise between the achievable η and the target thickness, which in part determines the gas load on the system. For example, from Fig. 1 we see that for a 200-keV D^+ beam one can achieve an η of 15% at $\pi = 1.5\times10^{16}$ molecules/cm^2, whereas 3.5×10^{16} molecules/cm^2 are required to raise η to 18%. When the η vs π curve has a maximum (for example, D^- in Fig. 1) the choice of target thickness is unambiguous. To provide a basis for comparison, we arbitrarily define the "optimum" neutralizer thickness as the value of π for which a maximum value of η is obtained, if a significant maximum exists; otherwise it is the value of π required to achieve 95% of the equilibrium η. The optimum neutralizer thickness vs energy is shown in Fig. 3. The curves for the positive ions cross over at about 75 keV/deuteron; above this energy the molecular ions can be neutralized with thinner targets than can the D^+ ions.

From the figures we see that D^- looks the best at higher energies, both in the attainable neutralization efficiency and the target thickness required to achieve that efficiency. Since no one has yet produced an intense negative-ion beam at high energies, the rest of the discussion will deal exclusively with positive beams.

3. MIXED BEAMS

Positive ion beams extracted from a deuterium plasma generally contain a mixture of all three positive ions, so a realistic analysis of neutralization efficiences requires the solution of Eqs. (1)-(3) and a knowledge of the ion-species composition of the extracted ion beam.

Of particular interest to us was the composition of the beam produced by the LBL 10-ampere neutral beam source [3]. In this source approximately 15 A of positive deuterium ions are extracted in 30 msec pulses at 20 keV from a 7-× 7-cm slotted array. The ions are neutralized in the beam line adjacent to the source by collisions with D_2 gas streaming from the source chamber. The beam strikes a calorimeter located 3.3 meters from the extractor; about 9.5 equivalent amperes of energetic ions and neutrals (the beam is about 90% neutral) are contained within a 10×20 cm section of the colorimeter.

The composition of the beam was measured with the experimental arrangement shown in Fig. 4 by sampling a portion of the beam striking the calorimeter through a 4.5 mm-diam aperture. Two independent measurements were possible with this arrangement: (1) With the sweep magnet removed and the gas cell evacuated, the ions remaining in the beam were analyzed in the magnet; (2) with the sweep magnet in place the ions were swept out of the beam, some of the neutrals were ionized in the gas cell, and then analyzed in the magnet. The results of either of these two measurements were used with Eqs. (1)-(3) to determine the composition of the ion species extracted from the source.

When the source was operated with D_2 gas, the composition of the neutral components of the beam with a neutralizer thickness of $7 \times 10^{15}/cm^3$ was typically 57% 20-keV D^0, 21% 10-keV D^0, 19% 6.7-keV D^0, 1% 20-keV D_2^0, and 2% 13-keV D_2^0. This corresponds to an ion composition in the extracted beam of 75% D^+, 15% D_2^+, and 10% D_3^+. Alteration of the composition by a change in ion-source operating conditions has been explored only to a limited extent; for example,

when arc parameters were changed while the total beam power to the calorimeter plate was kept constant, it was possible to raise the D_2^+ fraction to 22% (67% D^+, 22% D_2^+, and 11% D_3^+), but it was not possible to increase the D^+ fraction appreciably.

When hydrogen was used in the source, the measured fractions were 60% H^+, 20% H_2^+, and 20% H_3^+.[1]

The beam composition of the scaled-up 50-A source [3] is probably similar but has not been measured yet. Other kinds of high-current-density ion sources, for example, the ORNL "duoPIGatron" [4], also produce mixed-species beams.

Unwanted ion species can, in principle, be rejected at low energy by a magnetic selection process. However, to minimize space-charge blowup, present high-power-density beam systems have the neutralizer immediately following the last element of the extraction system. Consequently, no momentum selection of the ions is possible and the neutral beam (which represents about 90% of the beam power at 20 keV) is produced from all three ions.

In the near future, CTR experiments will require multi-megawatt beams at energies higher than 20 keV. One approach toward attaining higher energy beams is by the addition of acceleration stages to present-day sources; since post-acceleration will not alter the extracted-ion composition, it is of interest to consider the neutralization efficiencies for such beams. We have used the 20 keV hydrogen- and deuterium-beam compositions measured for the LBL source and with Eqs. (1)-(3) calculated the neutral components that could be achieved at 40, 80, and 160 keV with a hydrogen or deuterium neutralizer.

The results of the calculations, normalized to 1 MW of power in the full-energy atomic component, are presented in the form of flow diagrams in Fig. 5. At each energy a neutralizer thickness sufficient to obtain 95% of the equilibrium yield of full-energy H^0 or D^0 was used in the calculations. The power contained in the charged components and in the other neutral components (full-energy molecules and lower-energy atoms and molecules) is also shown. The neutral particle penetration thickness, P. T. (ions/cm^2), in a fusion-experiment plasma is a function of the particle energy, so the lower-energy neutrals will not penetrate as far as those at full energy; we have used penetration thicknesses given by Sweetman [5] to estimate a mean relative penetration thickness, $\langle$P. T$\rangle$, for the lower-energy neutral components.

4. DISCUSSION

In Fig. 5 we show examples of power flow in neutral beam systems, assuming initial ion compositions found experimentally for the LBL sources operated at 20 keV. Since collision fragments from the molecular ions have distinct energies, these flow diagrams can readily be modified by the reader for any other ion composition of the initial beam.

For these examples we assume that the accelerator optics are good enough that there is no beam loss on collimators; besides decreasing the useful neutral power, collimator interception could cause heating and impurity problems.

All of our calculations were carried out for hydrogen or deuterium neutralizers. Although the necessary cross sections are not available to survey the entire periodic table, sample calculations indicate that no significant gains in efficiency can be expected for the common gases.

Nevertheless, other neutralizers may be desirable to minimize gas loads on the system: At high energies the cross sections (both for electron-capture and loss) for higher-Z targets are larger so that the optimum in the neutralization efficiencies can be obtained at lower target thicknesses. There are, however, at least two disadvantages in using neutralizers other than hydrogen or deuterium: (1) The charged beam may suffer space-charge blowup in the drift region to the neutralizer, and (2) care must be taken to prevent gas from the neutralizer from entering the ion source (where it would be ionized and contribute to beam impurities) or the confined plasma.

Inspection of Fig. 5 shows that, for the examples shown, deuterium beams are neutralized more efficiently than hydrogen beams; this results from the higher atomic fraction and the lower speed of the deuterium beams. The neutralization efficiency decreases with increasing energy, and the very low neutral conversion obtained for 160-keV H beams (equivalent to 320 keV/deuteron in Fig. 2) draws attention to the need for high-power negative ion beams which can be neutralized more efficiently.

Even at the lowest accelerator voltage shown, significant fractions of the beams emerging from the optimized neutralizers are charged and/or at energies less than correspond to the full acceleration voltages. For example, to obtain 1 MW of 20 keV H^0 atoms requires 2.12 MW of power in the accelerated ion beam, of which 0.42 MW of ions and 0.71 MW of neutrals other than 20 keV H^0 atoms emerge from the neutralizer. The neutral components with less than full energy may

or may not be desirable in a given experiment, but we note two possible disadvantages: First, the lower-energy components may make experiments more difficult (for example, energy-equilibration time measurements). Second, since the neutral particle penetration thickness (ions/cm^2) is approximately proportional to the neutral particle energy for a given species [5], lower-energy neutrals will be trapped at larger radii, and may be lost rapidly to walls (for example, by charge exchange) or limiters.

The economic desirability of recovering the energy of the surviving ion beam, for example by electrostatic deceleration [6, 7] is apparent; from an engineering standpoint this will be much easier if all of the ions have the same momentum. Other possible ways to reduce energy losses in the charged component are by recirculation through the neutralizer [8].

The possibility of having nearly monoenergetic neutral atomic beams is clearly desirable, and the need for research toward this end is indicated. There may be ways to enhance the D^+ fraction in an ion source, for example, by constructing the arc chamber and gas feed lines of heated tungsten; but for the present, realistic mixtures of species must be considered when mating neutral beam systems with CTR confinement devices.

ACKNOWLEDGMENTS

The particle analyzer was fabricated in the mechanical shops of L. A. Biagi and H. H. Hughes. E. B. Hewitt and J. E. Galvin were in charge of source operation during data acquisition. We greatly appreciate their support.

FOOTNOTES

*This work was performed under the auspices of the U. S. Atomic Energy Commission.

[1]The higher atomic-ion yield with deuterium may be due to lower thermal speeds and, consequently, longer residence times of the heavier deuterium ions and atoms in the discharge. If tritium were used in the source we might expect an even larger atomic-ion fraction.

REFERENCES

[1] SWEETMAN, D. R., et al., in Plasma Physics and Controlled Nuclear Fusion Research 1971, IAEA, Vienna (1971) Vol. III, p. 393, Section 2.4.

[2] Data are taken from the compilation by ALLISON, S. K., GARCIA-MUNOZ, M., in Atomic and Molecular Processes (BATES, D. R., Ed.) Academic Press (1962); SWEETMAN, D. R., Proc. Roy. Soc. (London) A256 (1960) 416, and ORNL-3113 Rev. (1964) pp. 17 and 70; PIVOVAR, L. I., et al., Sov. Phys.-JETP 13 (1961) 23; KUPRIANOV, S. E., et al., Zh. Tek. Fiz. 33 (1963) 1252; McCLURE, G. W., Phys. Rev. 130 (1963) 1852, Phys. Rev. 140 (1965) A769, Phys. Rev. 153 (1967) 182; WILLIAMS, J. F., DUNBAR, D. N. F., Phys. Rev. 149 (1966) 62; BERKNER, K. H., et al., Phys. Rev. A 8 (1973) 2870.

[3] BAKER, W. R., et al., in Proceedings of the 5th Symposium on Engineering Problems of Fusion Research, Princeton, N. J., IEEE (1973) 413.

[4] STEWART, L. D., et al., "Neutral Beam Injection Heating of ORMAK", in Proceedings of the Third International Symposium on Toroidal Plasma Confinement, Garching, 1973.

[5] SWEETMAN, D. R., Nucl. Fusion 13 (1973) 157.

[6] MOIR, R. W., et al., in Plasma Physics and Controlled Nuclear Fusion Research 1971, IAEA, Vienna (1971) Vol. III, p. 315.

[7] FUMELLI, M., "Intense Fast Atom Beam Production with a

Grounded Large Area Ion Source, "Fontenay-aux-Roses Report EUR-CEA-FC-716 (1973), unpublished; submitted to Nuclear Instruments and Methods.

[8] BEAL, J. W., NEIL, B. K., Lawrence Livermore Laboratory Report UCRL-75605 (1974), unpublished; submitted to Nucl. Fusion.

TABLE CAPTION

TABLE I. CROSS SECTIONS FROM THE LITERATURE [2] USED IN THE CALCULATIONS (10^{-17} cm^2/D_2 MOLECULE). MOST ENTRIES WERE OBTAINED FROM MEASUREMENTS IN H_2 GAS WITH HYDROGEN PROJECTILES OF ONE-HALF THE TABULATED ENERGIES.

FIGURE LEGENDS

FIG. 1. Neutralization efficiency η [(power in neutral beam)/(power in initial ion beam)] vs D_2 neutralizer thickness for each of the four beams; 200-keV D^+, 400-keV D_2^+, 600-keV D_3^+, and 200-keV D^-.

FIG. 2. Maximum neutralization efficiency in D_2 vs beam energy, for each of the four beams, D^+, D_2^+, D_3^+, and D^-.

FIG. 3. "Optimum" neutralizer thickness for neutral production vs beam energy for each of the beams D^+, D_2^+, D_3^+, and D^-. Where no maximum in η vs π exists we choose π for 95% of equilibrium η.

FIG. 4. Schematic of apparatus to analyze charge- and neutral-beam composition.

FIG. 5. Power flow diagrams for 1 MW 20-, 40-, 80-, and 160-keV H^0 and D^0 injection systems. (The ion species composition of an LBL source has been assumed.) Estimates for relative penetration thicknesses [P. T. ($ions/cm^2$)] in a fusion-experiment were obtained from Sweetman [5].

TABLE I.

Energy keV/deut	D^+		D^0		D^-		D_2^+			D_2^0			D_3^+			
	σ_{10}	σ_{1-1}	σ_{01}	σ_{0-1}	σ_{-10}	σ_{-11}	$\sigma_{D_2^0}$	σ_{D^0}	σ_{D^+}	$\sigma_{D_2^+}$	σ_{D^0}*	σ_{D^+}	$\sigma_{D_2^0}$	$\sigma_{D_2^+}$	σ_{D^0}	σ_{D^+}
10	83	0.13	8.0 [b]	1.6	100	8.5	46	74	22	7.7	25	3.3	35	11	72	11
20	80	0.45	9.3 [a]	2.5	108	9.0	36	83	22	12	(17)	4.9	41	12.5	91	16
50	47	0.80	13	1.6	85	8.5	16	63	24	19	(9.5)	7.0	30	10.8	83	21
100	17	0.10	14	0.75	65	8.0	4.3	35	24	19	(7.3)	6.9	10	8.2	50	24
200	2.5 [a]	0.01	10.8	(0.25)	47	(5.3)	0.7	13 [c]	19	15	5.0	5.8	3.5	5.6	25	22.3
500	0.046 [a]	(0)	6.0	(0.06)	25	(2.2)	(0.04)	3.7 [c]	10	7.0	3.2	3.8	1.1	3.0	13	15
1000	0.0012	(0)	3.3	(0.02)	15	(0.75)	(0.006)	2.0 [c]	5.6	4.2	2.2	2.4	0.63	1.8	6.5	7
Estimated uncertainties	±10%	±30%	±10%	±20%	±15%	±10%	±10%	±10%	±20%	±20%	±25%	±25%	±20%	±15%	±10%	±10%

Estimated uncertainties are as shown under each column except as noted.

[a] ±15%

[b] +10-50%

[c] ±20%

() Parentheses indicate extrapolations or interpolations where no uncertainty can be assigned.

σ_{ij} (i,j = 1,0,-1) indicates cross section for change from charge state i to j.

σ_{D^0}, σ_{D^+}, etc. symbolize cross sections for the production of D^0, D^+, etc.

*Reaction $D_2^0 \rightarrow D^0 + D^+$ only.

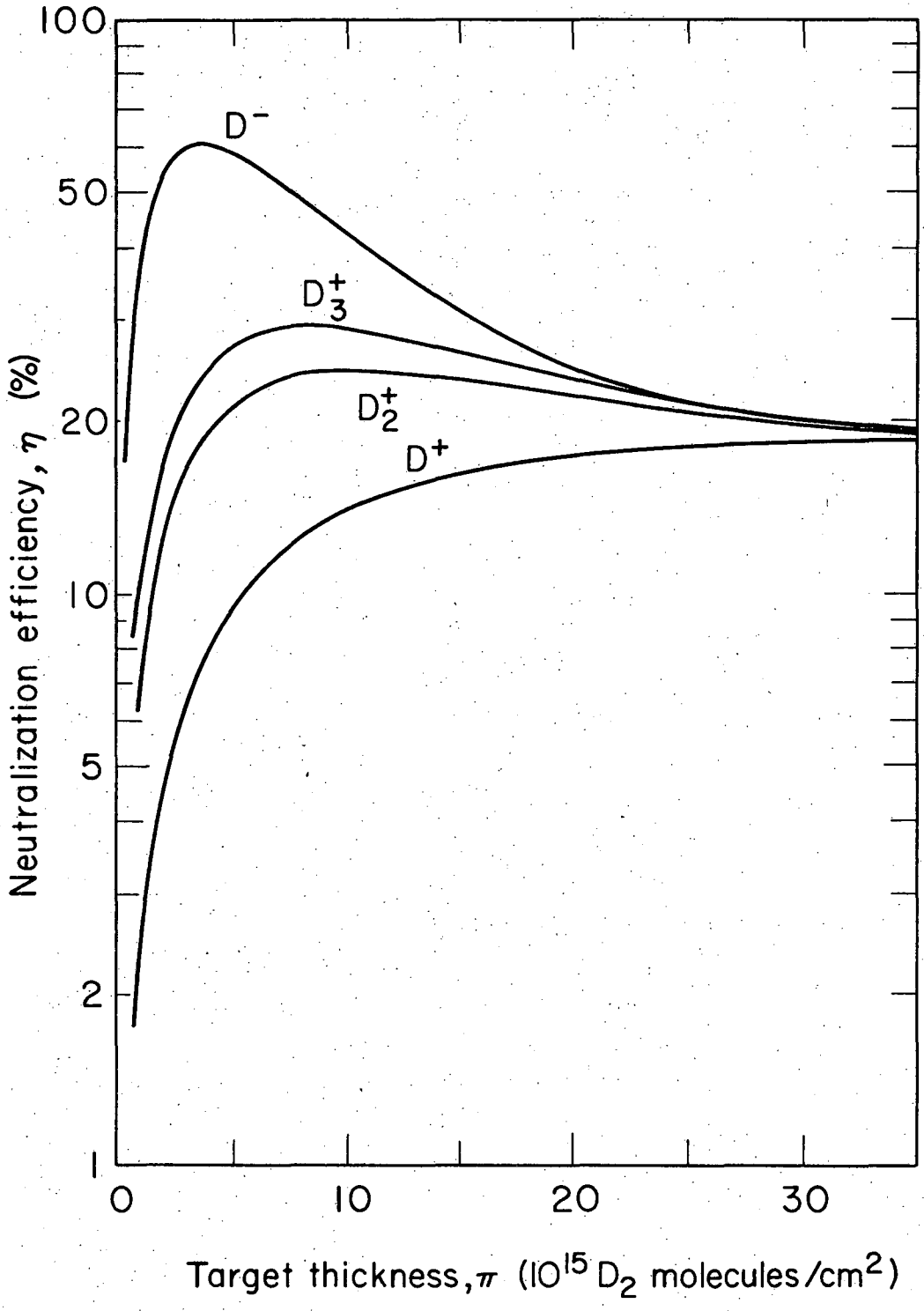

XBL 743-2708

Fig. 1.

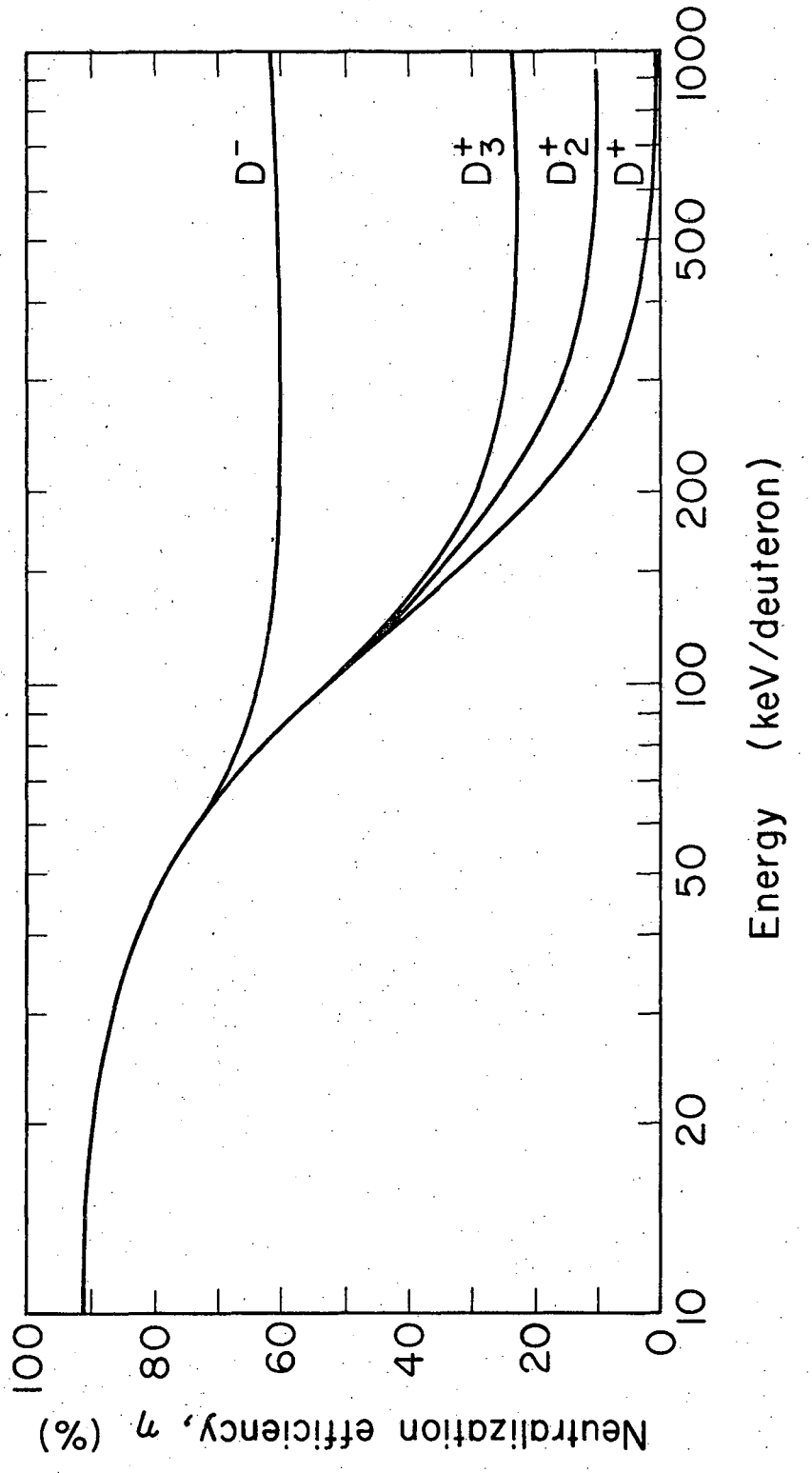

XBL 743-2709

Fig. 2.

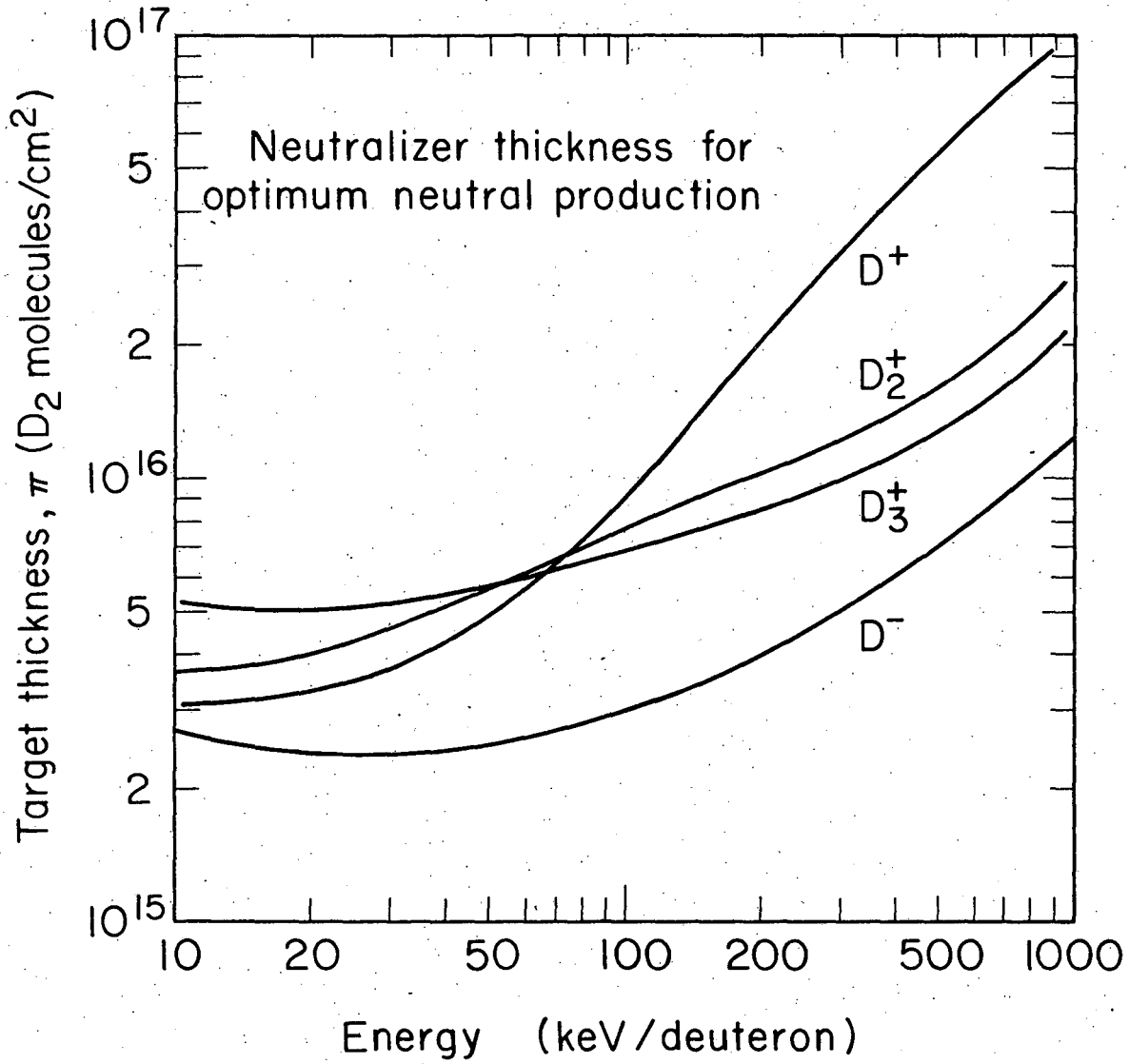
Neutralizer thickness for optimum neutral production
Target thickness, π (D2 molecules/cm2)
Energy (keV/deuteron)
D+
D2+
D3+
D−
10^17
5
2
10^16
5
2
10^15
10
20
50
100
200
500
1000
XBL746-3406

Fig. 3.

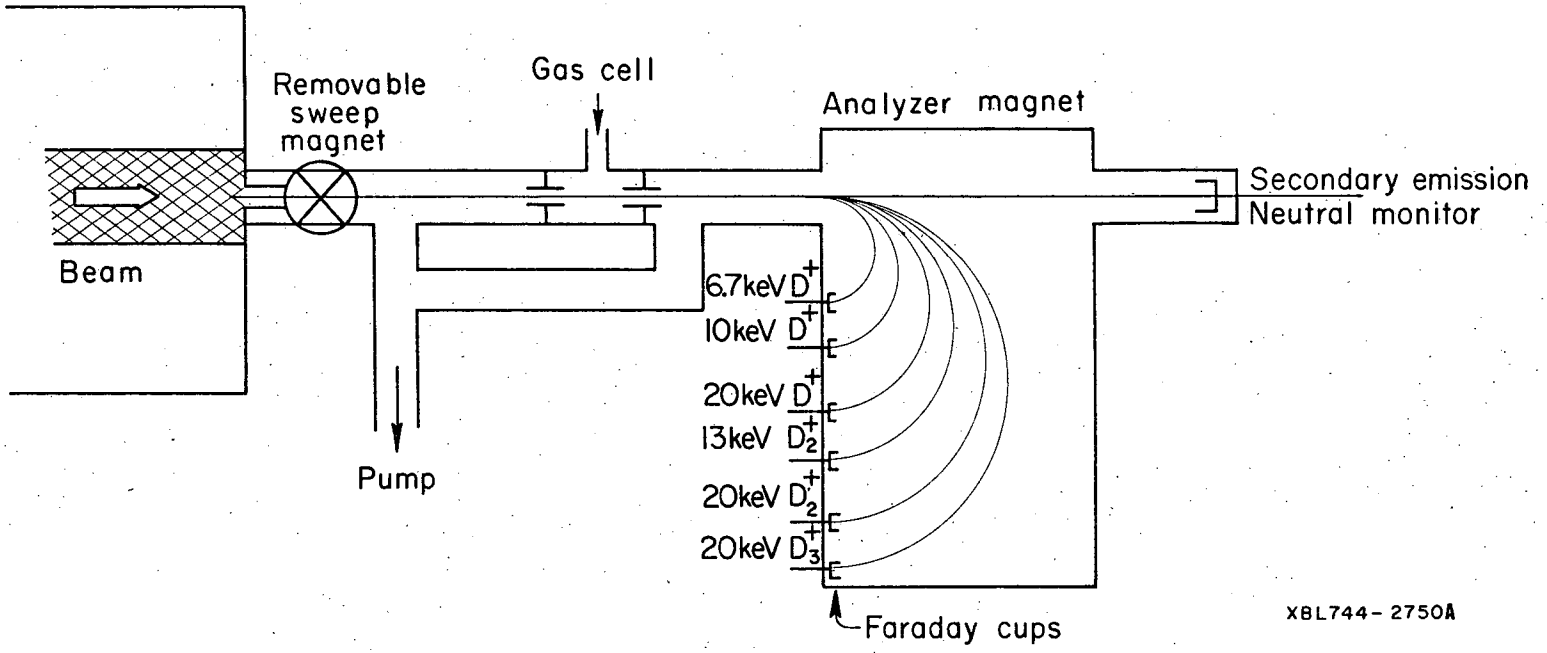
Removable
sweep
magnet
Gas cell
Analyzer magnet
Secondary emission
Neutral monitor
Beam
Pump
6.7keV D+
10keV D+
20keV D+
13keV D2+
20keV D2+
20keV D3+
Faraday cups
XBL744-2750A

Fig. 4.

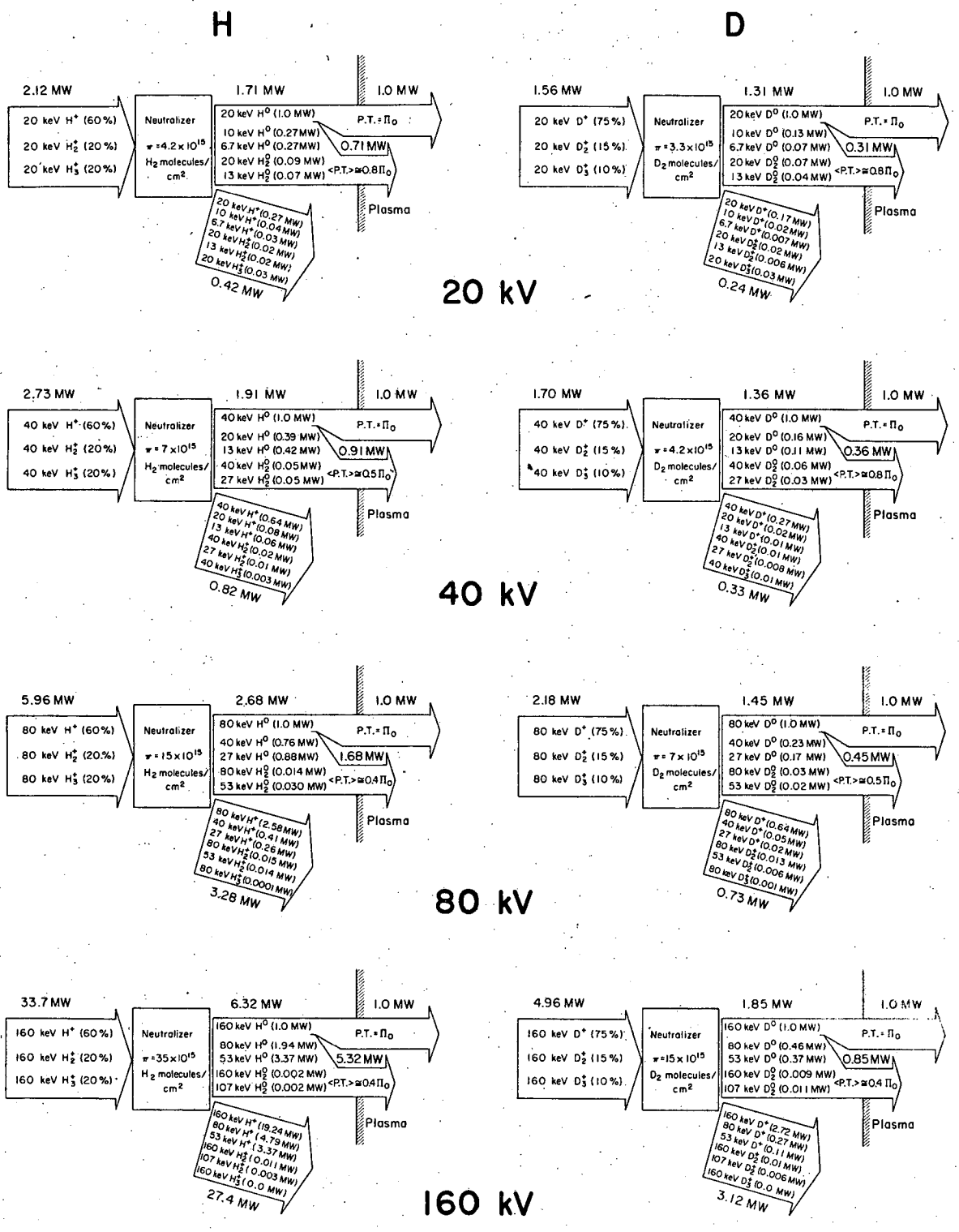
H
D
2.12 MW
20 keV H+ (60%)
20 keV H2+ (20%)
20 keV H3+ (20%)
Neutralizer
π=4.2×10^15
H2 molecules/cm2
1.71 MW
20 keV H0 (1.0 MW)
10 keV H0 (0.27MW)
6.7 keV H0 (0.27MW)
20 keV H2 (0.09 MW)
13 keV H2 (0.07 MW)
P.T.=Π0
0.71 MW
<P.T.>≅0.8Π0
1.0 MW
Plasma
20 keV H+(0.27 MW)
10 keV H+(0.04 MW)
6.7 keV H+(0.03 MW)
20 keV H2+(0.02 MW)
13 keV H2+(0.02 MW)
20 keV H3+(0.03 MW)
0.42 MW
1.56 MW
20 keV D+ (75%)
20 keV D2+ (15%)
20 keV D3+ (10%)
Neutralizer
π=3.3×10^15
D2 molecules/cm2
1.31 MW
20 keV D0 (1.0 MW)
10 keV D0 (0.13 MW)
6.7 keV D0 (0.07 MW)
20 keV D2 (0.07 MW)
13 keV D2 (0.04 MW)
P.T.=Π0
0.31 MW
<P.T.>≅0.8Π0
1.0 MW
Plasma
20 keV D+(0.17 MW)
10 keV D+(0.02 MW)
6.7 keV D+(0.007 MW)
20 keV D2+(0.02 MW)
13 keV D2+(0.006 MW)
20 keV D3+(0.03 MW)
0.24 MW
20 kV
2.73 MW
40 keV H+ (60%)
40 keV H2+ (20%)
40 keV H3+ (20%)
Neutralizer
π=7×10^15
H2 molecules/cm2
1.91 MW
40 keV H0 (1.0 MW)
20 keV H0 (0.39 MW)
13 keV H0 (0.42 MW)
40 keV H2 (0.05 MW)
27 keV H2 (0.05 MW)
P.T.=Π0
0.91 MW
<P.T.>≅0.5Π0
1.0 MW
Plasma
40 keV H+(0.64 MW)
20 keV H+(0.08 MW)
13 keV H+(0.06 MW)
40 keV H2+(0.02 MW)
27 keV H2+(0.01 MW)
40 keV H3+(0.003 MW)
0.82 MW
1.70 MW
40 keV D+ (75%)
40 keV D2+ (15%)
40 keV D3+ (10%)
Neutralizer
π=4.2×10^15
D2 molecules/cm2
1.36 MW
40 keV D0 (1.0 MW)
20 keV D0 (0.16 MW)
13 keV D0 (0.11 MW)
40 keV D2 (0.06 MW)
27 keV D2 (0.03 MW)
P.T.=Π0
0.36 MW
<P.T.>≅0.8Π0
1.0 MW
Plasma
40 keV D+(0.27 MW)
20 keV D+(0.02 MW)
13 keV D+(0.01 MW)
40 keV D2+(0.01 MW)
27 keV D2+(0.008 MW)
40 keV D3+(0.01 MW)
0.33 MW
40 kV
5.96 MW
80 keV H+ (60%)
80 keV H2+ (20%)
80 keV H3+ (20%)
Neutralizer
π=15×10^15
H2 molecules/cm2
2.68 MW
80 keV H0 (1.0 MW)
40 keV H0 (0.76 MW)
27 keV H0 (0.88MW)
80 keV H2 (0.014 MW)
53 keV H2 (0.030 MW)
P.T.=Π0
1.68 MW
<P.T.>≅0.4Π0
1.0 MW
Plasma
80 keV H+(2.58MW)
40 keV H+(0.41 MW)
27 keV H+(0.26 MW)
80 keV H2+(0.015 MW)
53 keV H2+(0.014 MW)
80 keV H3+(0.0001 MW)
3.28 MW
2.18 MW
80 keV D+ (75%)
80 keV D2+ (15%)
80 keV D3+ (10%)
Neutralizer
π=7×10^15
D2 molecules/cm2
1.45 MW
80 keV D0 (1.0 MW)
40 keV D0 (0.23 MW)
27 keV D0 (0.17 MW)
80 keV D2 (0.03 MW)
53 keV D2 (0.02 MW)
P.T.=Π0
0.45 MW
<P.T.>≅0.5Π0
1.0 MW
Plasma
80 keV D+(0.64 MW)
40 keV D+(0.05 MW)
27 keV D+(0.02 MW)
80 keV D2+(0.013 MW)
53 keV D2+(0.006 MW)
80 keV D3+(0.001 MW)
0.73 MW
80 kV
33.7 MW
160 keV H+ (60%)
160 keV H2+ (20%)
160 keV H3+ (20%)
Neutralizer
π=35×10^15
H2 molecules/cm2
6.32 MW
160 keV H0 (1.0 MW)
80 keV H0 (1.94 MW)
53 keV H0 (3.37 MW)
160 keV H2 (0.002 MW)
107 keV H2 (0.002 MW)
P.T.=Π0
5.32 MW
<P.T.>≅0.4Π0
1.0 MW
Plasma
160 keV H+ (19.24 MW)
80 keV H+ (4.79 MW)
53 keV H+ (3.37 MW)
160 keV H2+ (0.01 MW)
107 keV H2+ (0.003 MW)
160 keV H3+ (0.0 MW)
27.4 MW
4.96 MW
160 keV D+ (75%)
160 keV D2+ (15%)
160 keV D3+ (10%)
Neutralizer
π=15×10^15
D2 molecules/cm2
1.85 MW
160 keV D0 (1.0 MW)
80 keV D0 (0.46 MW)
53 keV D0 (0.37 MW)
160 keV D2 (0.009 MW)
107 keV D2 (0.011 MW)
P.T.=Π0
0.85 MW
<P.T.>≅0.4Π0
1.0 MW
Plasma
160 keV D+(2.72 MW)
80 keV D+(0.27 MW)
53 keV D+(0.1 MW)
160 keV D2+(0.01 MW)
107 keV D2+(0.006 MW)
160 keV D3+(0.0 MW)
3.12 MW
160 kV
XBL 746-3550

Fig. 5.

TECHNICAL INFORMATION DIVISION
LAWRENCE BERKELEY LABORATORY
UNIVERSITY OF CALIFORNIA
BERKELEY, CALIFORNIA 94720